scientific reports



OPEN

Improved acid-driven inhibition of effector T cell function by a pHLIP variant-conjugated PD-L1

Hang Zheng^{1,2,5}, Mianjing Wang^{1,2,5}, Junjuan Feng^{1,2,5}, Yuting Zhang², Haiyan Wu², Min Zhang², He Xiao², Chunxia Qiao², Jing Wang², Longlong Luo², Xinying Li², Jiannan Feng², Yuangiang Zheng^{1⊠}, Yi Wang^{3™}, Dongsheng Sheng^{4™} & Guojiang Chen^{2™}

Programmed cell death-ligand 1 (PD-L1)/PD-1 axis is crucial for maintenance of immune homeostasis and its impairment partially accounts for the pathogenesis of inflammatory diseases. Hence, augmenting PD-L1/PD-1 signals represents a novel strategy to prevent destructive inflammation and induce immune tolerance. Recently, we developed a new cargo by conjugating the ectodomain of PD-L1 with pHLIP, a low pH-responding and membrane-inserting peptide, and demonstrated its potent immune-suppressive activity under weakly acidic (pH6.1) conditions in vitro. Herein, we further showed that PD-L1-pHLIP (termed as PD-L1-pHLIP at not meakly acidic buffer, but not in nearly neutral pH (pH6.8) solutions. To overcome this obstacle, pHLIP was replaced by a variant harboring two mutations (Asp14Gla and Asp25Aad) and PD-L1 ectodomain was conjugated to the N-terminus of pHLIP variant via sulfo-SMCC linker (termed as PD-L1-pHLIP_{va}). PD-L1-pHLIP_{va} potently inhibited T effector function including proliferation, activation as well as proinflammatory cytokine release in nearly neutral pH buffer through PD-L1/PD-1 interaction. The inhibitory function of PD-L1pHLIP_{us} was attributed to more amounts of PD-L1 anchored on the surface of several types of immune cells compared with PD-L1-pHLIP_{wr}. Given that the niche in the lesions of inflammation is weakly acidic even nearly neutral pH, PD-L1-pHLIP_{va} represents a new arsenal to potentially dampen excessive inflammatory reactions.

Keywords PD-L1, pHLIP_{va}, Acidity, T cell, Immunosuppression

PD-L1, a ligand for (PD)-1, is expressed by CD4⁺ and CD8⁺ T cells, B cells, dendritic cells, macrophages, and nonhemopoietic tissues^{1,2}. The interaction between PD-L1 and PD-1 inhibits T cell activation and plays an important role in maintenance of immune homeostasis and resolution of inflammation^{3,4}. There is mounting evidence that the impairment of PD-L1/PD-1 signals contributes largely to the pathogenesis of autoimmunity and inflammatory diseases, making it rational to develop PD-1 agonists as therapeutics against unresolved inflammation^{5,6}.

pH (Low) Insertion Peptides (pHLIPs) are a family of soluble \sim 36 amino acid peptides, which are monomeric and largely unstructured at neutral and high pH 7 . If the environment is acidic, pHLIPs fold and insert across the plasma membrane to form a stable transmembrane helix, thus facilitating to transport the payloads into cytosolic compartment or display an antigenic peptide on the cell surface when the payloads or peptides are tethered at the C or N terminus of pHLIPs $^{8-11}$. Recently, we have developed a new cargo by engaging the ectodomain of murine PD-L1 to the N terminus of pHLIPs, and demonstrated its potent immune-suppressive activity under acidic conditions in vitro 12 . Mechanistically, PD-L1-pHLIP $_{\rm wt}$ is decorated smoothly on the surface of cells in acidic buffer instead of neutral aqueous solution and thereby delivers negative signals to effector T cells by PD-L1/PD-1 interaction. Of note, the pH $_{50}$ of membrane insertion of pHLIP $_{\rm wt}$ utilized in our work is approximately 6.1 10,13,14 , rendering the possibility that PD-L1-pHLIP $_{\rm wt}$ is unable to anchor on the cellular membrane in the surroundings with relatively high or near neutral pH and thereby loses its immune-suppressive function. To address this issue, the function of PD-L1-pHLIP was evaluated in pH6.8 and 6.1 buffer respectively in this study.

¹Research Center of Molecular Biology, School of Basic Medical Sciences, Inner Mongolia Medical University, Hohhot 010058, Inner Mongolia, China. ²Institute of Pharmacology and Toxicology, Beijing 100850, China. ³Department of Hematology, The Fifth Medical Center, Chinese PLA General Hospital, Beijing 100071, China. ⁴Department of Thoracic surgery, The Fifth Medical Center, Chinese PLA General Hospital, Beijing 100071, China. ⁵Hang Zheng, Mianjing Wang and Junjuan Feng contributed equally to this work. [∞]email: zhengyq688@163.com; yk091023@163.com; shenqdongshenq1978@163.com; jyk62033@163.com

As expected, PD-L1-pHLIP actively suppressed lymphocyte expansion in pH6.1 solution. While, the inhibitory function was lost in pH6.8 buffer. Furthermore, to retain the immune-suppressive ability of PD-L1-pHLIP in pH6.8 buffer, a pHLIP variant was utilized, in which Asp14 and Asp 25 were replaced by γ -carboxyglutamic acid and α -aminoadipic acid respectively ¹⁵. PD-L1 was fused to N-terminus of this variant via sulfo-SMCC linker. Consequently, this novel construct displayed prominent inhibitory capacity to lymphocyte proliferation and proinflammatory mediators release in pH6.8 as well as 6.1 buffer.

Results

PD-L1-pHLIP_{wt} inhibits T effector function in pH6.1 rather than pH6.8 buffer

Firstly, we determined the inhibitory effects of PD-L1-pHLIP_{wt} on T cell responses upon TCR stimulation under nearly neutral pH (pH6.8) and weakly acidic (pH6.1) conditions respectively. In consistent with our previous $study ^{12}, soluble\ PD-L1-pHLIP_{wt}\ did\ not\ exhibit\ the\ suppressive\ function\ on\ lymphocyte\ proliferation\ in\ neutral$ aqueous solution, whereas actively suppressed lymphocyte expansion in pH6.1 buffer titrated by lactic acid (Fig. 1a). In contrast, PD-L1-Fc or control protein had no inhibitory effects (Fig. 1a, data not shown). Intriguingly, PD-L1-pHLIP_{vot} lost its inhibitory function on anti-CD3/CD28-stimulated polyclonal proliferation of lymphocyte in pH6.8 buffer (Fig. 1a). Higher doses of PD-L1-pHLIP $_{\rm wt}$ also had no effects on lymphocyte expansion in neutral or pH6.8 buffer (Fig. S1a, b). To accurately clarify the inhibitory effects of PD-L1-pHLIP_{wt} on T cell subsets, carboxyfluorescein diacetate succinimidyl ester (CFSE) dilution was performed. PD-LÏ-pHLIP, indeed, significantly suppressed CD4⁺ and CD8⁺T cell expansion in pH6.1 buffer (Fig. 1b). However, the inhibitory effects were not observed in pH6.8 solutions (Fig. 1b). In accord with this, PD-L1-pHLIP_{ust} decreased IFN-γ and IL-2 secretion by lymphocytes in pH6.1 buffer instead of pH6.8 solutions (Fig. 1c). Furthermore, the effects of PD-L1-pHLIP_{wt} on inhibition of lymphocyte proliferation and proinflammatory cytokine production were dosedependent (Fig. 1d, e). Next, we detected the effects of PD-L1-pHLIP_{wt} on the expression of T cell activation biomarkers (e.g. CD25 and CD69). Under acidic conditions, TCR stimulation enable increased expression of CD25 and CD69 on CD4 $^+$ T cells and PD-L1-pHLIP $_{
m wt}$ treatment reduced their expression levels in pH6.1 rather than pH6.8 buffer (Fig. 1f). We also evaluated the inhibitory function of PD-L1-pHLIP $_{
m wt}$ in hydrochloric acid-titrated pH6.1 and 6.8 buffer. Similar results were seen (Fig. S2a, b). To determine the function of PD-L1-pHLIP, on antigen-specific T cell expansion, CD4+T cells were isolated from OT II-transgenic mice and pulsed with OVA₃₂₃₋₃₃₉-loading accessory cells. Lactic acid treatment had no significant influence on CD4⁺T cell proliferation. Importantly, PD-L1-pHLIP_{wt} dramatically reduced OVA-pulsed T cell expansion in pH6.1 buffer but not in pH6.8 solutions (Fig. 1g). Therefore, we make a conclusion that PD-L1-pHLIP, displays its immuno-suppressive function under weakly acidic conditions, which is lost under nearly neutral pH conditions. This may be attributed to the fact that in nearly neutral pH buffer, PD-L1-pHLIP, wt is incapable of inserting into the cellular membrane and thereby can not crosslink to its ligand PD-1, which is prerequisite for initiation of PD-L1/PD-1 signals^{16,17}.

PD-L1-pHLIP_{wt} displays on the surface of several types of immune cells under acidic conditions

Our previous study has shown that PD-L1-pHLIP_{wt} had ability to span across the cellular membrane by conformation changes of pHLIP in response to low pH and retain on the surface of T and B cell lines and primary mouse and human lymphocytes¹². Accordingly, we further determined cellular distribution of PD-L1-pHLIP_{wt} in pH6.8 and 6.1 buffer. In agreement with previous study¹², no fluorescence was visible when PE-labeled PD-L1-pHLIP_{wt} was incubated with anti-CD3/CD28-stimulated lymphocytes in neutral aqueous solutions (data not shown). Unexpectedly, in pH6.8 buffer, fluorescence-labeled PD-L1-pHLIP_{wt} was easily seen on the surface of several types of lymphocytes including NK, dendritic cell, monocyte, macrophage and B cells (Fig. 2a). The magnitude of fluorescence was highest on B subset (Fig. 2a). Interestingly, the fluorescence on T lymphocyte was absent, indicating that PD-L1-pHLIP_{wt} could not insert into cellular membrane of this subset under acidic conditions, which was further supported by the inability of the insertion of PD-L1-pHLIP_{wt} in pH6.1 buffer (Fig. 2a). Notably, the intensity of fluorescence on immune cells detected by flow cytometry was significantly lower in pH6.8 buffer compared with that in pH6.1 solutions (Fig. 2b). This may account for distinct effects of PD-L1-pHLIP_{wt} in pH6.8 and 6.1 buffer as described above. The relatively low magnitude of PD-L1-pHLIP_{wt} on the cell surface in pH6.8 buffer is not sufficient to deliver negative signals to T cells and thereby inhibit effector function.

Construction of pHLIP variant conjugated with PD-L1

Recently, An and colleagues developed a pHLIP variant in which Asparate at the position of 14 and 25 was mutated to γ -carboxyglutamic acid (Gla) and α -aminoadipic acid (Aad) respectively (termed as pHLIP $_{va}$). pHLIP $_{va}$ showed a pH $_{50}$ of 6.79 and had improved pH-response 15 . Accordingly, PD-L1 ECD was conjugated to the N-terminus of the pHLIP $_{va}$ using sulfosuccinimidyl 4-(N-maleimidomethyl) cyclohexane-1-carboxylate (sulfo-SMCC) as a coupling linker (Fig. 3a). A cysteine (Cys, C) at the N-terminus of pHLIP $_{va}$ provides an exposed sulfhydryl group (-SH) so that pHLIP $_{va}$ (Fig. S3a, b) could be conjugated to the side chains of the lysine (Lys, K) residues on the PD-L1 ECD through sulfo-SMCC coupling 18,19 . According to matrix-assisted laser desorption ionization time of flight mass spectrometry (MALDI-TOF MS) results (Fig. S3c), one or more pHLIP $_{va}$ were conjugated to PD-L1, indicating successful synthesis of the PD-L1-pHLIP $_{va}$ molecules. Furthermore, sulfo-SMCC reaction sites at lysine (K) was detected via tandem mass spectrometry (MS/MS) (Table S1). It is necessary to compare the binding capacity of PD-L1-pHLIP $_{va}$ and aforementioned PD-L1-pHLIP $_{wt}$ to the ligands (i.e. anti-PD-L1 mAb and PD-1) to determine if PD-1/PD-L1 interaction is affected after the chemical conjugation. The results showed the comparable engagement with antibody or PD-1 protein between PD-L1-pHLIP $_{va}$ and PD-L1-pHLIP $_{wt}$ (Fig. 3b, c), indicating that the chemical conjugation has no or minimal effects on the PD-1/PD-L1 interaction.

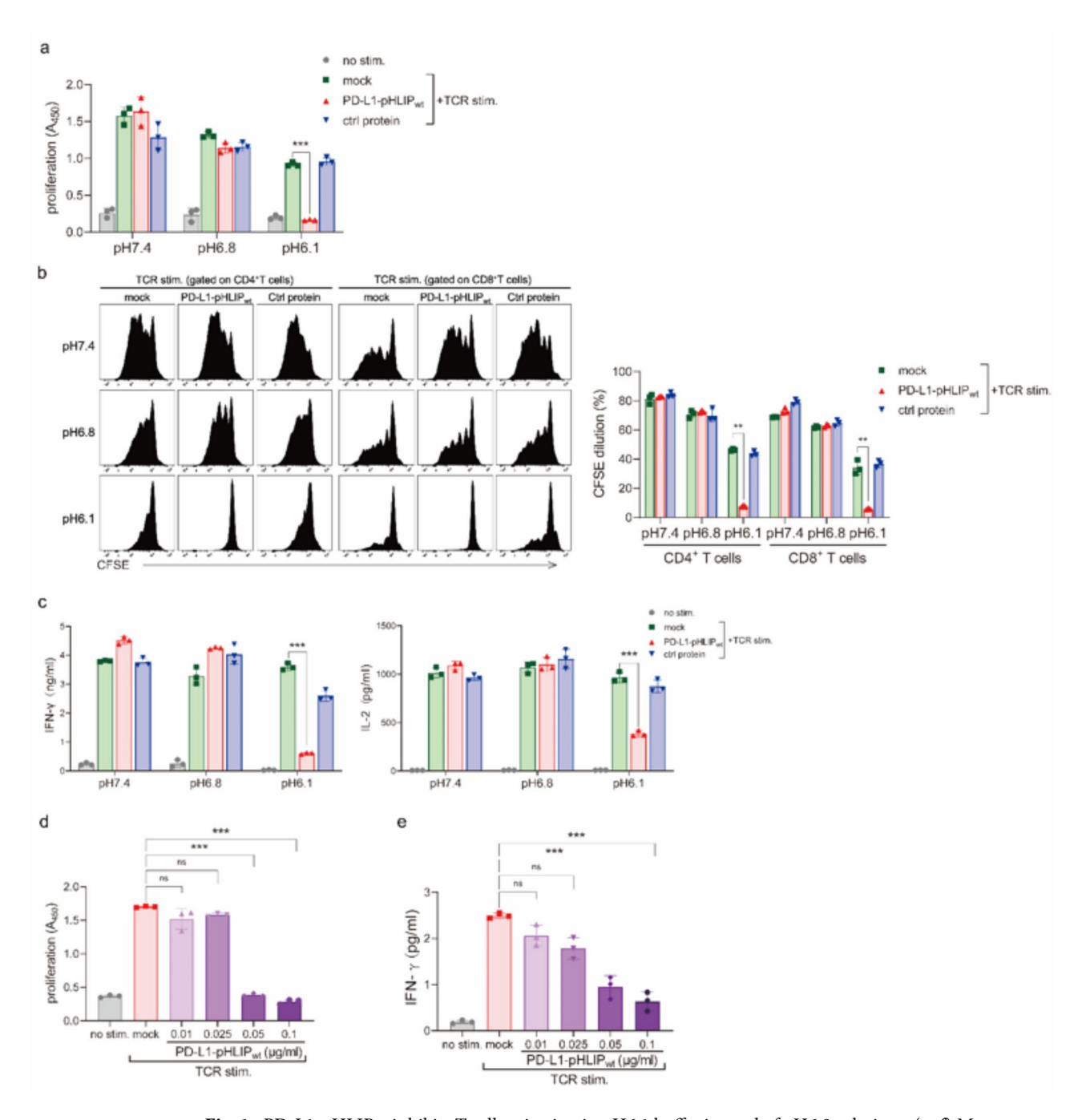


Fig. 1. PD-L1-pHLIP inhibits T cell activation in pH6.1 buffer instead of pH6.8 solutions. (a–f) Mouse lymphocytes were isolated from the spleen by Ficoll gradient centrifugation and stimulated with CD3/CD28 activator microbeads in the presence of soluble PD-L1-pHLIP or HER2-pHLIP (Ctrl protein) (0.1 μg/mL) for 72 h in the indicated lactate-titrated pH buffer. (a) The proliferation was determined by BrdU cell proliferation assay. (b) CD4⁺T cell population was gated and its proliferation was detected by CFSE dilution. (c) The supernatants were collected and IFN-γ as well as IL-2 production was examined by ELISA. (d,e) Soluble PD-L1-pHLIP at the indicated concentrations (0.01–0.1 μg/mL) was added. The proliferation and IFN-γ production were determined by BrdU cell proliferation assay or ELISA respectively. (f) CD4⁺T cells were gated and CD25 as well as CD69 expression in this population was examined by flow cytometry. (g) Splenic CD4⁺T cells from OT II-transgenic mice were fractionated by negatively magnetic isolation and cocultured with OVA_{323–339}-pulsed irradiated accessory cells for 72 h in the presence of soluble PD-L1-pHLIP or Ctrl protein (0.1 μg/mL) for 72 h in the indicated lactate-titrated pH buffer. The CD4⁺T cell proliferation was determined by BrdU cell proliferation assay. The experiments were repeated three or five times. The data was pooled from these experiments, and representative plots were shown. **p<0.01; ***p<0.001; ***p<0.001; *n.s no significance.

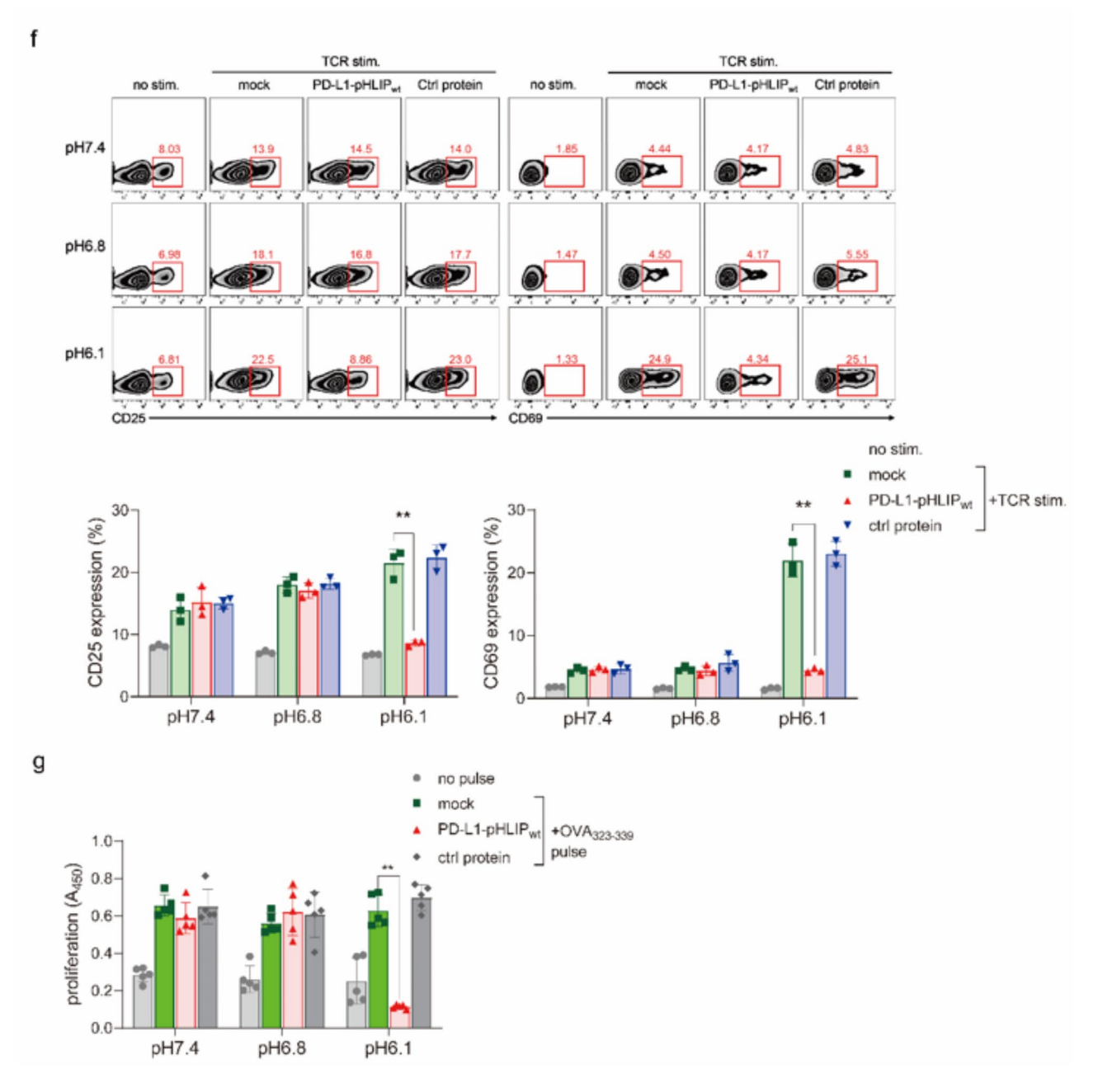


Figure 1. (continued)

PD-L1-pHLIP_{va} suppresses T effector response in pH6.8 as well as 6.1 buffer

Next, we compared the immune-suppressive function of PD-L1-pHLIP_{va} and PD-L1-pHLIP_{wt} in acidic solutions. Similar to PD-L1-pHLIP_{wt}, plate-coated PD-L1-pHLIP_{va} displayed strong inhibition of lymphocyte proliferation and IFN-γ production following TCR stimulation (Fig. S4a, b). Importantly, soluble PD-L1-pHLIP_{va} instead of PD-L1-pHLIP_{wt} actively inhibited T cell proliferation in lactic acid-titrated pH6.8 buffer (Fig. 4a). Moreover, the inhibitory ability of PD-L1-pHLIP_{va} in pH6.1 and 6.8 solutions was comparable (Fig. 4a). PD-L1-pHLIP_{va}'s function was attributed to the orchestrated cooperation between PD-L1 fragment and pHLIP_{va} because PD-L1 or pHLIP_{va} alone or their mixture or control protein-conjugated pHLIP_{va} showed no inhibition of T cell activation (Fig. 4b). CFSE dilution assays also identified the immune-suppressive function of PD-L1-pHLIP_{va} on CD4⁺ and CD8⁺T subsets in pH6.8 buffer respectively (Fig. 4c). Furthermore, the release of proinflammatory cytokines was blocked dramatically by PD-L1-pHLIP_{va} in pH6.8 buffer (Fig. 4d). A dose-dependent fashion on the inhibition of lymphocyte expansion and IFN-γ production by PD-L1-pHLIP_{va} was observed (Fig. 4e, f). T cell activation (CD25/69 expression) was also dampened by PD-L1-pHLIP_{va} in pH6.8 buffer (Fig. 4g). As described above, we further examined the inhibitory function of PD-L1-pHLIP_{va} on polyclonal human lymphocyte expansion and OVA-specific T cell proliferation respectively. As a consequence, PD-L1-pHLIP_{va} rather than PD-L1-pHLIP_{wt} potently suppressed T cell expansion upon anti-CD3/CD28 stimulation or OVA peptide pulse in

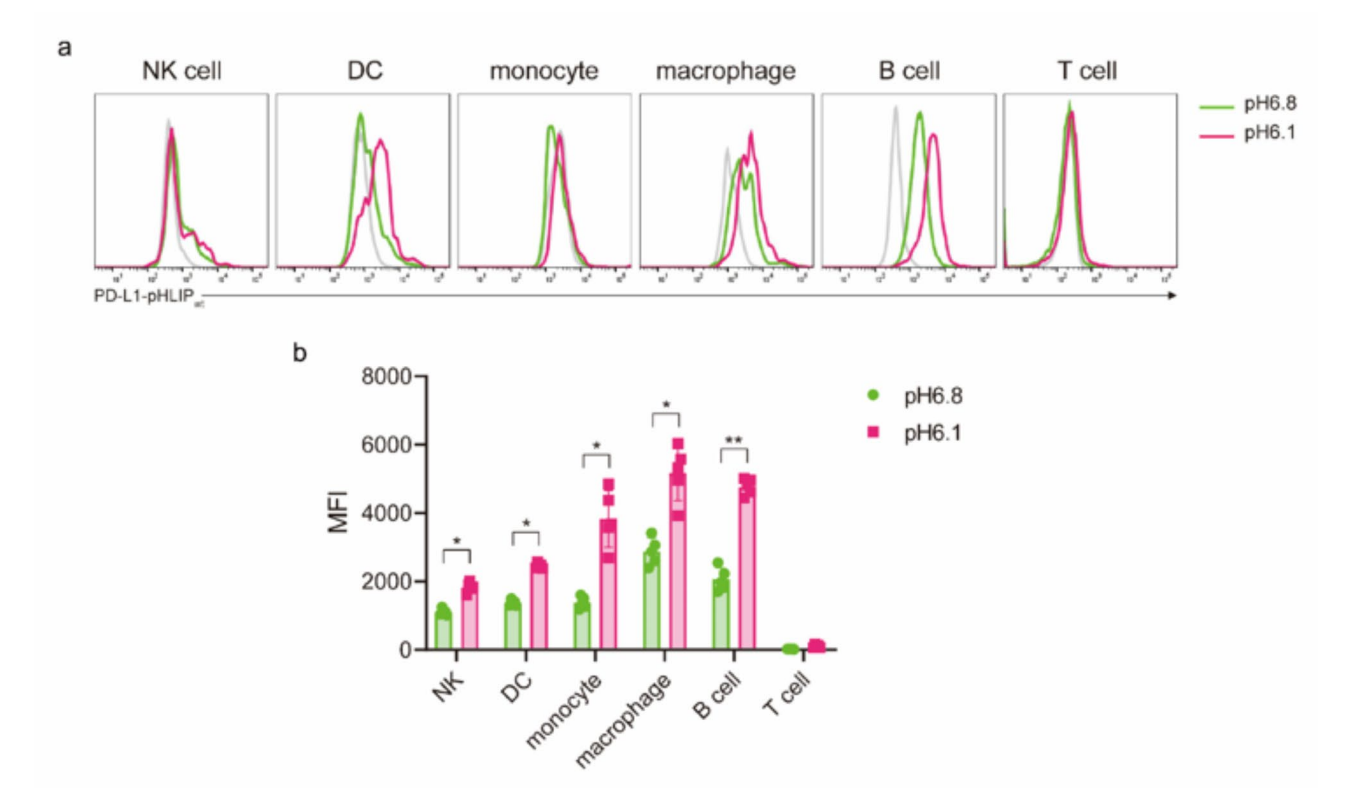


Fig. 2. PD-L1-pHLIP $_{\rm wt}$ is decorated on the surface of several types of immune cell subsets under acidic conditions. Mouse lymphocytes were stimulated with CD3/CD28 activator microbeads in the presence of PE-labeled soluble PD-L1-pHLIP $_{\rm wt}$ (0.1 µg/mL) for 72 h in pH6.8 or 6.1 buffer. The immune cell populations were gated by appropriate antibodies respectively and the PE fluorescence on these populations was detected by flow cytometry. (a) Representative plots. (b) The data pooled from five independent experiments. *p < 0.05; **p < 0.01.

pH6.8 buffer (Fig. 4h, i). It is noteworthy that, as we described previously, PD-1 expression on CD4⁺ and CD8⁺T cells was increased significantly upon TCR stimulation respectively and that the function of PD-L1-pHLIP $_{\rm wt}$ was dependent on PD-L1/PD-1 interaction¹². To determine whether PD-L1-pHLIP $_{\rm va}$ did likewise, an PD-1-specific antibody was utilized. The results showed that addition of anti-PD-1 mAbs almost entirely abrogated the ability of PD-L1-pHLIP $_{\rm va}$ to inhibit lymphocyte proliferation and proinflammatory mediator release (Fig. 4j, k). In addition, in HCl-titrated pH6.8 buffer, the inhibitory function of PD-L1-pHLIP $_{\rm va}$ was equal to that in lactic acid-titrated counterparts (Fig. S5a). As well, the effects were abolished by PD-1-specific antibody (Fig. S5b). We also determined the ability of PD-L1-pHLIP $_{\rm va}$ under neutral conditions. Somewhat unexpectedly, in pH7.0 or 7.2 buffer, PD-L1-pHLIP $_{\rm va}$ completely lost its proliferation-inhibiting function (Fig. S6).

PD-L1-pHLIP_{va} displays more abundantly on the surface of several types of immune cells than PD-L1-pHLIP_{wr} in pH6.8 buffer

We assumed that the potency of PD-L1-pHLIP $_{\rm va}$ to inhibit T effector function in nearly neutral pH solutions is due to the adequate amounts of PD-L1 anchored on the cellular membrane. Therefore, the abundance of PD-L1-pHLIP $_{\rm va}$ and PD-L1-pHLIP $_{\rm wt}$ on the surface of several types of immune cells indicated was compared according to the protocol described above. Similar to PD-L1-pHLIP $_{\rm wt}$, PE-labeled PD-L1-pHLIP $_{\rm va}$ was observed on the cellular membrane of NK, DC, monocyte, macrophage as well as B cells, instead of T cells, in pH6.8 buffer (Fig. 5a, c). Consistently, PD-L1-pHLIP $_{\rm va}$ was not found on the surface of T cells. Of importance, the magnitude of the fluorescence of PD-L1-pHLIP $_{\rm va}$ was stronger than that of PD-L1-pHLIP $_{\rm wt}$ (Fig. 5b), which may account for the inhibitory function of PD-L1-pHLIP $_{\rm va}$ instead of PD-L1-pHLIP $_{\rm wt}$ in pH6.8 buffer.

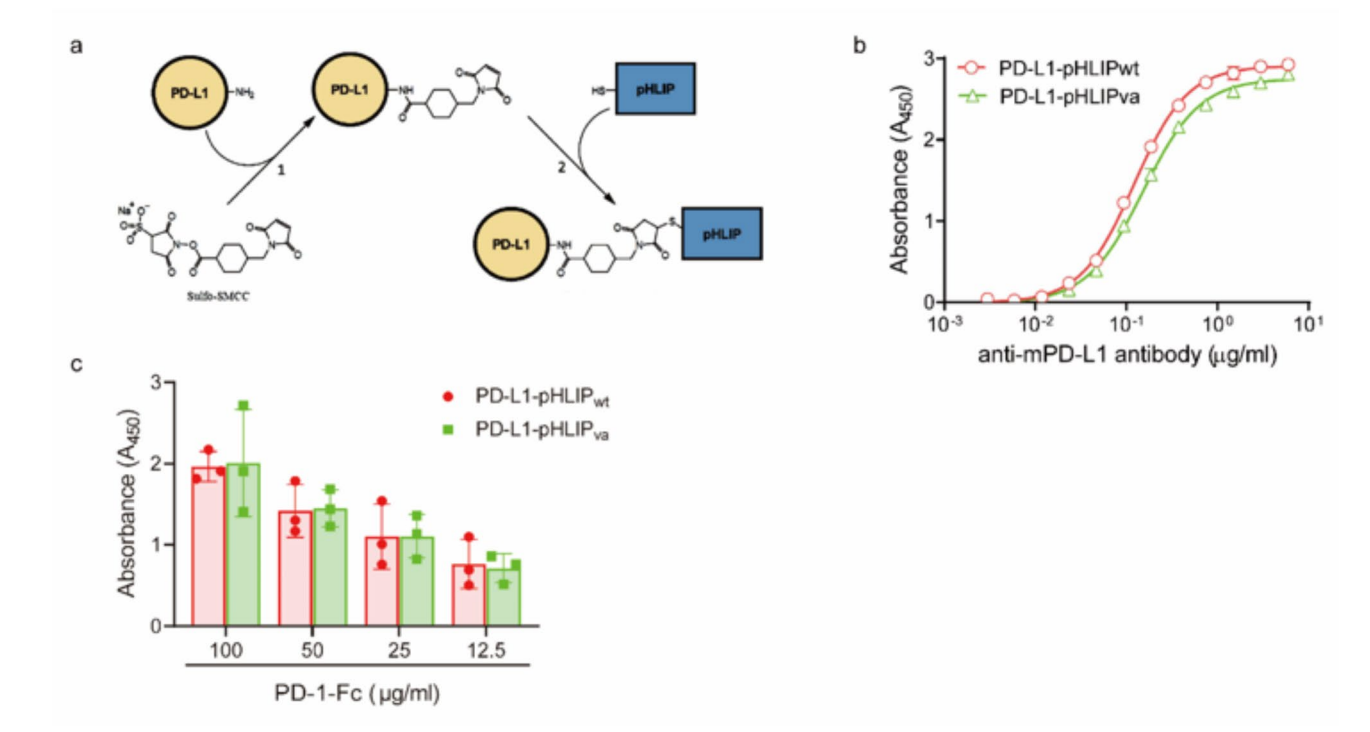


Fig. 3. Validation of the binding of PD-L1-pHLIP $_{\rm va}$ to anti-PD-L1 mAb and PD-1 protein. (a) Schematic illustration of assembly of pHLIP $_{\rm va}$ -conjugated PD-L1. (b) The binding capacity of PD-L1-pHLIP $_{\rm va}$ as well as PD-L1-pHLIP $_{\rm wt}$ to an anti-murine PD-L1 antibody was determined by ELISA. (c) The ability of PD-L1-pHLIP $_{\rm va}$ as well as PD-L1-pHLIP $_{\rm wt}$ to bind recombinant murine PD-1 protein was determined by ELISA. The data was pooled from three experiments.

Discussion

Hypoxia and innate immune cell activation by inflammatory factors and microbial products induce/boost anaerobic and aerobic glycolysis, increasing the production and release of lactate and concomitant acidification of the extracellular environment^{20,21}. Acidosis is thus a promising target for therapeutic intervention²². Our previous work has demonstrated that PD-L1 ectodomain tethering pHLIP_{wt} potently dampened immune response to TCR stimulation under weakly acidic conditions in vitro¹². In this study, we further confirmed that PD-L1-pHLIP_{wt} lost immune-suppressive function completely under nearly neutral pH conditions. Considering that the drop of pH in the niche of inflammation is assumed to be not dramatical and that an adaptive tissue response to inflammatory acidification occurs subsequently to promote pH homeostasis²³, unresponsiveness of this cargo to weak acidosis may hinder its application in vivo to dampen excessive inflammatory reactions. To resolve this issue, we further developed a new construct by tethering a pHLIP variant to the ectodomain of PD-L1 via chemical linking. This novel cargo displayed excellent inhibitory capacity to T cell effector function including proliferation, activation and proinflammatory mediator production under nearly neutral pH conditions (Fig. 6). It is noteworthy that T cell activation was accompanied by simultaneous elevation of PD-1 and PD-L1 expression levels on the cell surface, which was impaired upon addition of lactic acid (Fig. S7a, b)¹². The up-regulated expression of PD-1/PD-L1 appears to be an inherent braker to prevent over-activation of T cells, but not enough to dampen T cell response once upon TCR stimulation. Therefore, supplement of exogenous PD-L1 (i.e. PD-L1-pHLIP) fuels PD-1 signals to adequately inhibit T cell activation. To our knowledge, it is the first pHLIPbased immunomodulator to control T cell-mediated inflammatory activation through enhancing PD-1/PD-L1 signaling axis.

PD-L1-pHLIP $_{va}$ administration in the model of inflammatory diseases, however, remains challenging. Acidosis in the sites of inflammation is not permanent. Acute inflammatory responses are characterized by massive infiltration of PMN and lactate accumulation, leading to the rapid fall of local pH. As the states of inflammation turn from acute to chronic as well as an adaptive response to acidification occurs through augmenting the expression of ion exchange channel proteins (e.g. SLC26A3), pH rises to the nearly neutral. It has been proposed that once the pH rises rapidly from acidic to basic, pHLIP exits from the bilayer core, which proceeds approximately 400 times faster than folding/insertion²⁴. Therefore, PD-L1-pHLIP $_{va}$ might readily shed from the cellular membrane due to the dynamic alteration of pH in the lesions. One approach is to substitute a double-switch pHLIP for pHLIP $_{va}$, which harbors a unique hook-like switch to lock the peptide securely on the bilipid layer even if pH changes from acidic to neutral²⁵, rendering stable anchoring of PD-L1-pHLIP on the

surface of cells residing in the microenvironment of inflammatory diseases and thereby sustained inhibition of inflammatory responses. The validation of this concept is ongoing.

It is worthy to note that PD-L1-pHLIP had capacity to span across the membrane of several types of immune cells under acidic conditions, except for T cells. Further investigations are needed to assess the membraneinserting ability of PD-L1-pHLIP separately in each purified immune subsets, considering that in cell mixture the competitive binding of PD-L1-pHLIP probably occurs among different cells. In addition, it has been proposed that the interaction between pHLIP and the membrane lipid bilayer can be affected by membrane composition^{26,27}, asymmetry^{28–30}, and the local ionic environment³¹, using model systems of liposomes. Characterization of physical-chemical features of the membrane of T lymphocytes will thus be warranted to elucidate the inertness of this population to acid-driven insertion of pHLIP. In summary, this study constructed the second-generation PD-L1-pHLIP that represents a promising therapeutic candidate for T cell-triggered inflammatory diseases such as rheumatoid arthritis and type 1 diabetes 4,32,33. Its efficacy in murine models of these diseases is being evaluated.

Methods

 $\label{eq:synthesis} \textbf{Synthesis of PD-L1-pHLIP}_{va} \\ \textbf{For pHLIP coupling, sulfosucclnlmldyl 4-(N-malemldomethyl) cyclohexane-1-carboxylate (sulfo-SMCC)} \\$ (ThermoFisher, USA) (4800 nmol in 300 µL PBS) was added into murine PD-L1 ECD protein (prepared by our lab) solution in PBS (10 nmoL, 200 µL). The mixture was incubated in a 1.5 mL Eppendorf tube at room temperature for 2 h with gentle shaking, with a pH control at 7.4 at the whole process. The sulfo-SMCC conjugated PD-L1 (SMCC-PD-L1) were purified by NAP-5 column (GE Healthcare, UK) pre-equilibrated with PBS buffer. Subsequently, a total of 4800 nmoL pHLIP $_{\!\scriptscriptstyle \rm VA}$ (Ac-ACEQNPIYWARYAGlaWLFTTPLLLLAadLALLV DADEGT) (Chinese Peptide Inc. China) in PBS was added into the conjugated PD-L1 solution, and the reaction was incubated at room temperature for 5 h with gentle shaking. The resulting PD-L1-pHLIP_{va} was purified by NAP-10 column (GE Healthcare, UK) pre-equilibrated with PBS buffer. The same method was followed for HER2T276-652 (human HER2 ectodomain (276aa-652aa), prepared by our lab) coupling. The molecular weight of pHLIP, and PD-L1-pHLIP, was measured by matrix-assisted laser desorption ionization time of flight mass spectrometry (MALDI-TOF MS) (Bruke, Germany).

Tandem mass spectrometry (MS/MS) detection of sulfo-SMCC modification on PD-L1 segment

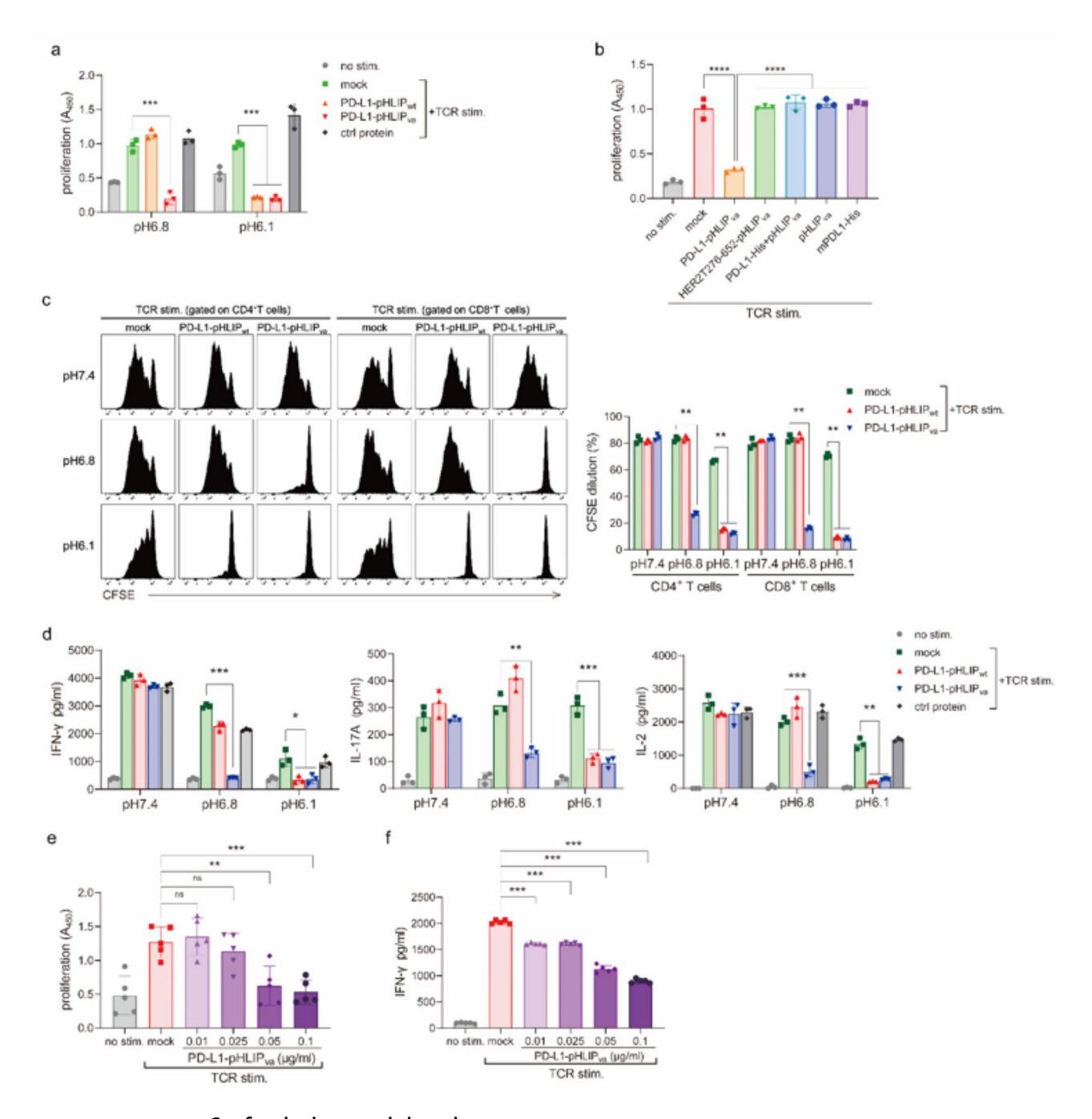
To track the binding sites of sulfo-MSCC modification, SMCC-PD-L1 was digested by trypsin (Promega, USA). The digested peptides were analyzed by a nano-LC-LTQ-Orbitrap XL MS/MS system. MS data were analyzed by Proteome Discoverer software (version 1.4.0.288, ThermoFisher). The second MS spectra were searched in the Mus database using the SEQUEST search engine. Sulfo-SMCC modification of lysine, glutathionylation, or oxidation of cysteine and oxidation of methionine were set as variable modifications.

Lymphocyte isolation and BrdU cell proliferation assays

The lymphocytes in the spleen of BALB/c mice (6-8 week old, male, obtained from Charles River, China) were isolated by Ficoll gradient centrifugation respectively. (These mice were maintained in specific pathogen-free conditions, and were euthanized by cervical dislocation by skilled laboratory animal practitioners with the certification.) Human PBMC were fractionated from healthy adult donors (participants in our experimental group recruited from March 29, 2023 to November 9, 2023) with signed written informed consents by gradient centrifugation. Lymphocytes (5×10⁵ cells/well) or PBMC (5×10⁴ cells/well) were stimulated with Dynabeads™ Mouse or human T-Activator CD3/CD28 beads (Cat. No. 11161D, 11452D, ThermoFisher, USA) for 72 h in the indicated pH buffer titrated by lactic acid or hydrochloric acid. For ovalbumin (OVA)-specific T cell stimulation, CD4+T cells were isolated from the spleen of OT-II mice (purchased from Cyagen Biosciences, China) by negative magnetic isolation kit (Cat. No. 130-104-454, Miltenyi Biotec, USA) and incubated with γ ray-irradiated accessory cells, which were prepared by depletion of T cells in syngeneic splenocytes using magnetic isolation kits (Cat. No. 130-094-973, Miltenyi Biotec), in the presence of OVA₃₂₃₋₃₃₉ (Cat. No. O1641, 10 μg/mL, Merk, USA) for 72 h. Coated or soluble recombinant proteins (PD-L1-pHLIP_{wt}, PD-L1-pHLIP_{va}, HER2T276-652-pHLIP_{va}, PD-L1, pHLIP_{va}; The endotoxin levels of these purified proteins were less than 0.1 EU/µg assayed by LAL method) were added at titrated concentrations simultaneously once upon initiation of TCR stimulation. BrdU cell proliferation assays were performed according to the manufacturer's protocols (Cat. No. 6813 S, CST, USA). In some settings, neutralizing mAbs against murine PD-1 or IgG2a isotypes (Cat. No. 135247, 400565, 10 μg/mL, Biolegend, USA) were added. The supernatant was collected and stored at -20 °C until analyzed.

CFSE dilution assays

Splenic lymphocytes were stained with 5 µM CFSE (Cat. No. c34554, ThermoFisher) in PBS for 10 min at 37 ℃ and then cells were washed two times with RPMI-1640 medium and resuspended at a concentration of 2.5×10^6 cells/mL. The CFSE-stained cells were transferred to 96-well plates (200 µL/well) and stimulated with Mouse T-Activator CD3/CD28 beads for 72 h in the indicated pH buffer. Simultaneously, PD-L1-pHLIP_{wt} or PD-L1pHLIP_{va} (0.1 μg/mL) was added. The cells were harvested and stained with APC-conjugated anti-mouse CD8 and FITC-conjugated anti-mouse CD4 (Cat. No. 100712, 100408, Biolegend) at 4 °C for 30 min and subsequently analyzed by flow cytometry.



Confocal microscopic imaging

T and B cells were isolated from the spleen of mice by negatively magnetic isolation kits (Cat. No. 130-095-130, 130-090-862, Miltenyi Biotec) respectively and placed in a laser confocal dish (NEST, Wuxi, China), and then cultured overnight. Biotinylated PD-L1-pHLIP $_{\rm va}$ was added at 5 µg/mL and cultured at 37 °C for 1 h. Cells were washed twice with PBS with corresponding pH and then FITC-conjugated avidin (Cat. No. 405101, Biolegend) was added and cultured for 30 min. The fluorescence on the cellular membrane was observed under confocal laser scanning microscope (Andor, Dragonfly 200).

∢Fig. 4. PD-L1-pHLIP_{so} inhibits T cell activation in pH6.1 and 6.8 solutions. (a-g,j,k) mouse lymphocytes were stimulated with CD3/CD28 activator microbeads in the presence of soluble PD-L1-pHLIP_{wt}, PD-L1pHLIP_{va} or Ctrl protein (0.1 μg/mL) for 72 h in the indicated lactate-titrated pH buffer. (a) The lymphocyte proliferation was determined by BrdU cell proliferation assay. (b) Soluble Her2T276-652-pHLIP, pHLIP, or PD-L1 protein (0.1 µg/mL) as controls were added parallelly. The lymphocyte proliferation was determined by BrdU cell proliferation assay. (c) CD4+ and CD8+ T cell populations were gated respectively and their proliferation was detected by CFSE dilution. (d) The supernatants were collected and IFN-γ, IL-17 A as well as IL-2 levels were examined by ELISA. (e,f) PD-L1-pHLIP_{va} at the indicated concentrations was added. The lymphocyte proliferation and IFN-γ production in the supernatants was determined by BrdU cell proliferation assay and ELISA respectively. (g) CD4⁺T and CD8⁺T cells were gated respectively. CD25 and CD69 expression in these two populations was examined by flow cytometry. (h) Human PBMC were stimulated with CD3/ CD28 activator microbeads in the presence of soluble PD-L1-pHLIP $_{\!\scriptscriptstyle WI}$, PD-L1-pHLIP $_{\!\scriptscriptstyle VI}$ or Ctrl protein (0.1 µg/mL) for 72 h in the indicated lactate-titrated pH buffer. The lymphocyte proliferation was determined by BrdU cell proliferation assay. (i) CD4+T cells were isolated from OT II-transgenic mice and co-cultured with OVA $_{323-339}$ -pulsed accessory cells for 72 h in the presence of soluble PD-L1-pHLIP $_{\rm wt}$, PD-L1-pHLIP $_{\rm tot}$, PD-L1-pHLIP $_{\rm tot$ or Ctrl protein (0.1 μg/mL) in the indicated pH buffer. The T cell proliferation was determined by BrdU cell proliferation assay. (j,k) Monoclonal antibodies to PD-1 or isotypes (10 μg/mL) were added in the culture. The lymphocyte proliferation was determined by BrdU cell proliferation assay. IFN-y production in the supernatants was examined by ELISA. The experiments were repeated 3 or 5 times. The data were pooled from these experiments, and representative plots were shown. *p < 0.05; **p < 0.01; ****p < 0.001; ****p < 0.0001; ****p < 0.0001; **** significance.

ELISA

A total of 96-well plate was coated overnight with PD-L1-pHLIP wt or PD-L1-pHLIP (2 μ g/mL), washed three times with PBS-T, and blocked with 4% nonfat dried milk in PBS for 1 h at room temperature. Twofold serial dilution of anti-murine PD-L1 antibody (Cat. No. 124338, Biolegend) from 6 μ g/mL was added. For murine PD-1-Fc (prepared in our lab), it was added at 12.5, 25, 50, 100 μ g/mL and incubated for 1 h at room temperature. The wells were washed and HRP-conjugated anti-murine Fc IgG1 (Cat. No. A16084, 1:1,000, Thermofisher) in 0.5% BSA was added and incubated for 1 h at room temperature. A TMB substrate kit (Invitrogen, USA) was used for detection at 450 nm. IFN- γ , IL-2, IL-17 A levels in the supernatants were determined by commercial ELISA assay kits (Cat. No. 430807, 431007, 432504, Biolegend).

Flow cytometry

PD-L1-pHLIP wa and PD-L1-pHLIP was labeled by PE dye with Conjugation Kit, according to manufacturer's protocol (Cat. No. 102918, Abcam, UK) and incubated at 0.1 μ g/mL with mouse lymphocytes in the presence of Mouse T-Activator CD3/CD28 beads for 72 h in pH6.8 or 6.1 buffer. Single cell suspensions (1×10⁶) were stained on ice for 30 min with PE-conjugated anti-murine CD25 (Cat. No. 101903, Biolegend), APC-conjugated anti-murine CD69 (Cat. No. 104513, Biolegend) and PE-conjugated anti-murine PD-L1 (Cat. No. 124307, Biolegend) in FACS buffer (PBS, 1% BSA, and 1 mM EDTA). Flow cytometry was performed on a FACSAria II (BD Biosciences) and data analysis was performed by using the FlowJo software.

Statistical analysis

Data were expressed as the mean \pm SEM, and the differences between groups were analyzed using either unpaired two-tailed Student's t test or one-way ANOVA with Bonferroni correction. A value of p < 0.05 was considered statistically significant.

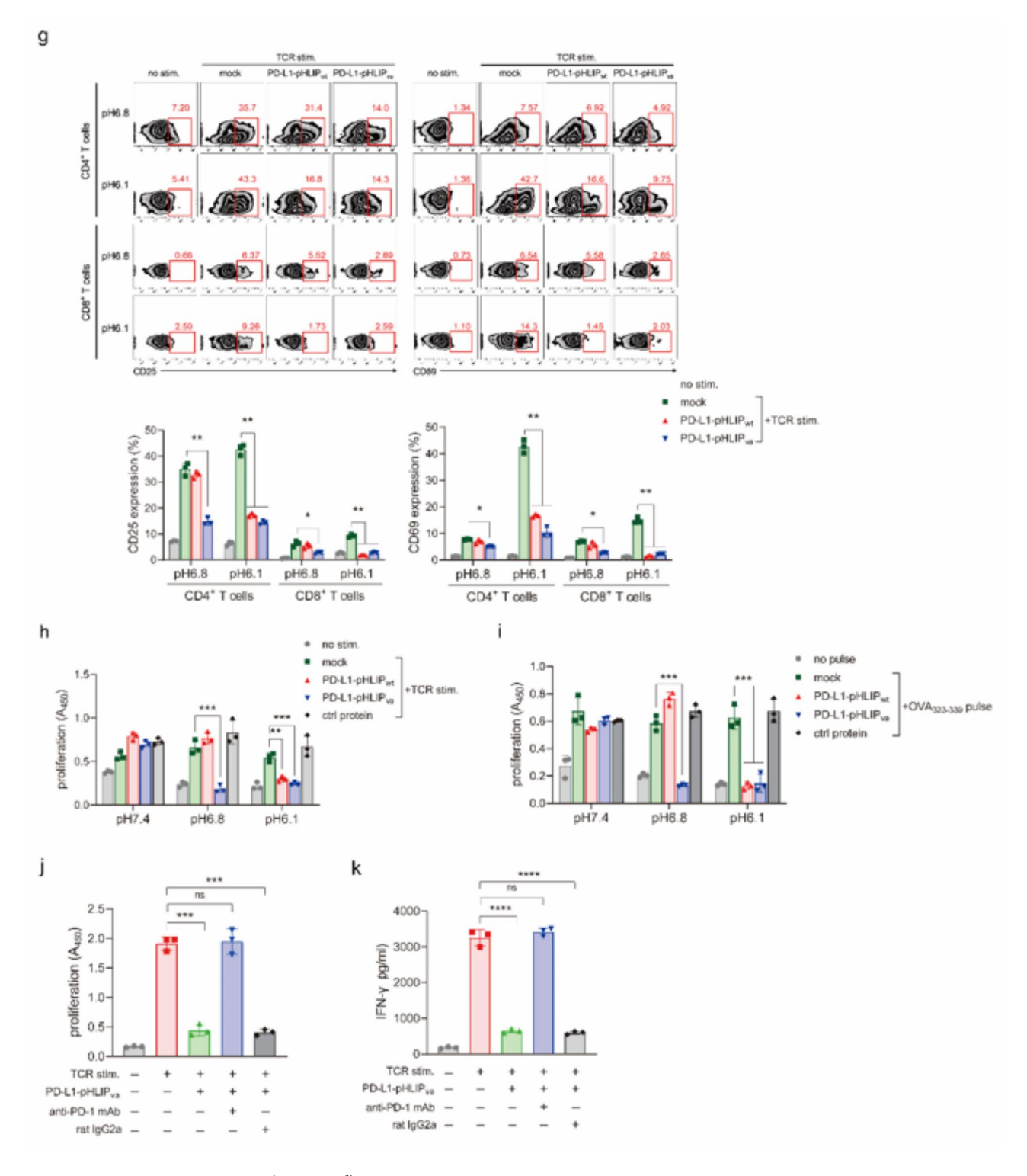


Figure 4. (continued)

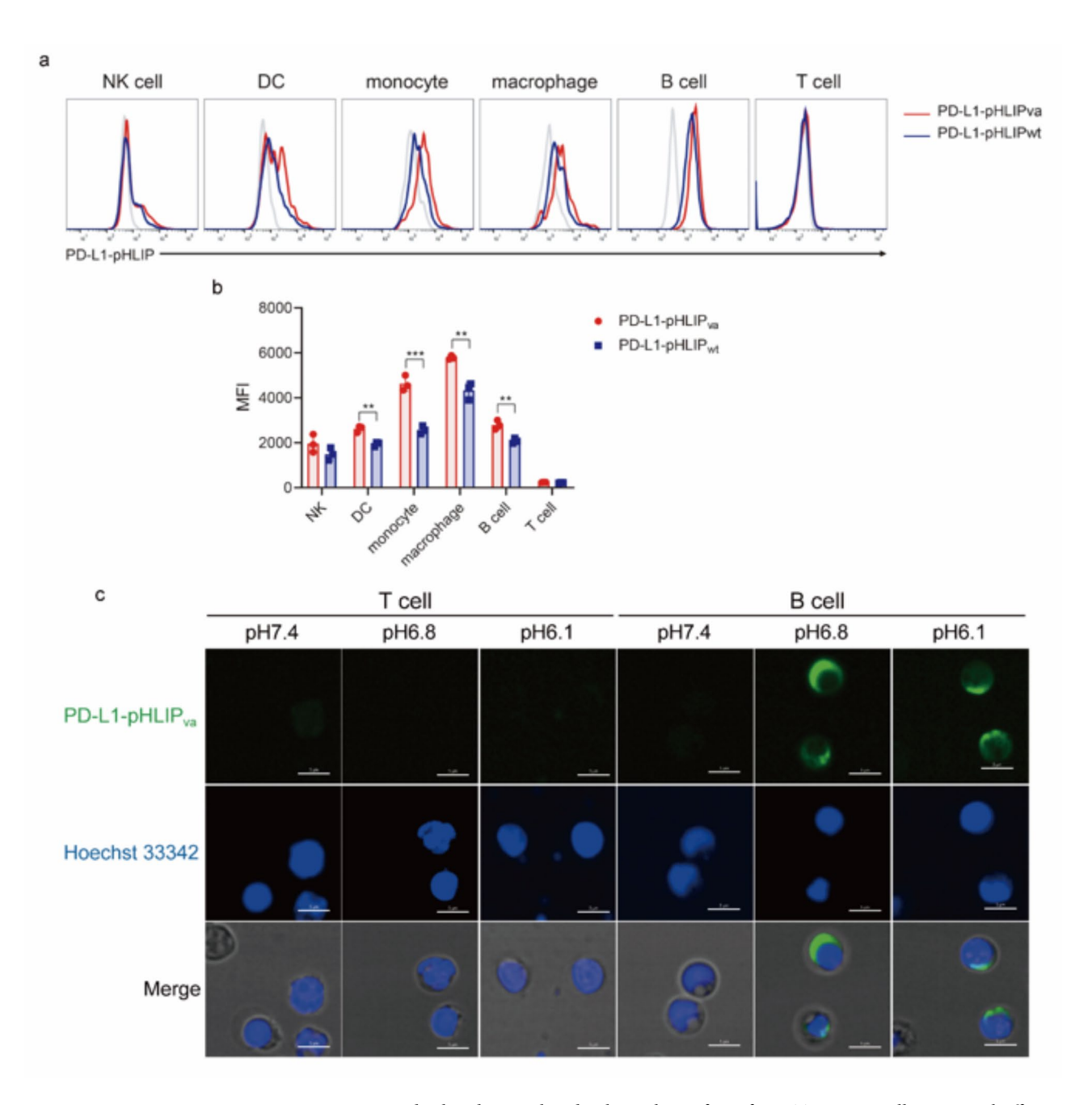
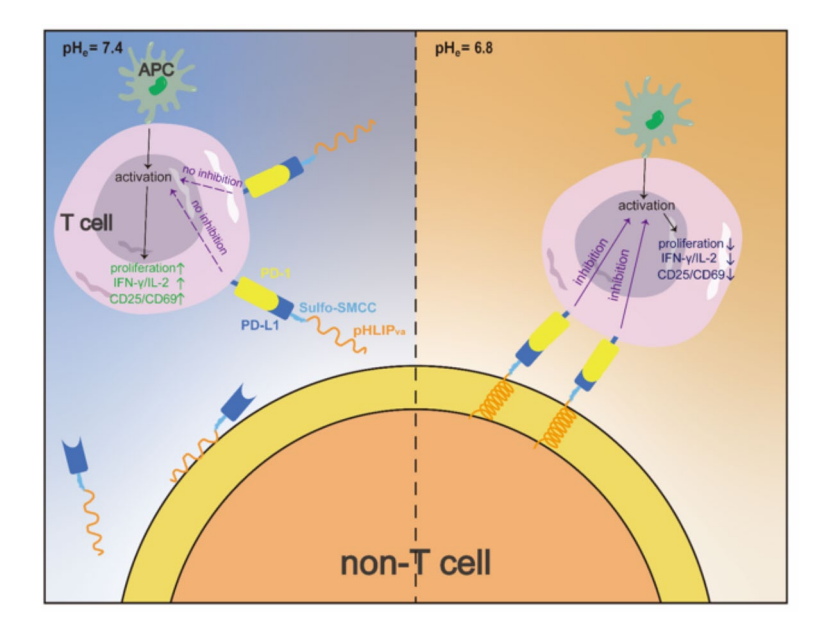


Fig. 5. PD-L1-pHLIP $_{va}$ is displayed more abundantly on the surface of non-T immune cells in pH6.8 buffer. (a,b) Mouse lymphocytes were stimulated with CD3/CD28 activator microbeads in the presence of PE-labeled soluble PD-L1-pHLIP $_{va}$ and -pHLIP $_{wt}$ (0.1 µg/mL) for 72 h in pH6.8 buffer. The immune cell populations were gated by appropriate antibodies respectively and the PE fluorescence on these populations was detected by flow cytometry. (c) Biotinylated PD-L1-pHLIP $_{va}$ (5 µg/mL) was incubated with magnetically isolated B or T cells in pH7.4, 6.8 or 6.1 for 1 h, respectively. FITC-conjugated avidin was added and the insertion into membrane was examined by fluorescence microscopy. Scale: 5 µm. (a,c) Representative plots or imaging. (b) The data pooled from three independent experiments. **, p<0.01; ***, p<0.001.



 $\textbf{Fig. 6}. \ \ \text{The schematic illustration on the mode of action of PD-L1-pHLIP}_{va}. \ \ \text{PD-L1-pHLIP}_{va}, \ \text{chemically of the schematic illustration}$ ligating a pHLIP variant to the ectodomain of PD-L1 via sulfo-SMCC linker, has potency to actively inhibit T effector response via delivering PD-L1/PD-1 signals by spanning across the cellular membrane of neighboring non-T cells under nearly neutral conditions (pH6.8), while this cargo cannot insert into membrane in pH7.4 buffer, leading to the loss of immunosuppressive function.

Data availability

The original data presented in the study are included in the article and the supplementary materials. For further inquiries, please directly contact the corresponding author.

Received: 6 January 2025; Accepted: 9 April 2025 Published online: 18 April 2025

References

- 1. Greenwald, R. J., Freeman, G. J. & Sharpe, A. H. The B7 family revisited. Annu. Rev. Immunol. 23, 515-548. https://doi.org/10.114 6/annurev.immunol.23.021704.115611 (2005).
- 2. Kuol, N., Stojanovska, L., Nurgali, K. & Apostolopoulos, V. Pd-1/Pd-L1 in disease. Immunotherapy 10, 149-160. https://doi.org/10 .2217/imt-2017-0120 (2018).
- 3. Qin, W. et al. The diverse function of Pd-1/Pd-L pathway beyond cancer. Front. Immunol. 10, 2298. https://doi.org/10.3389/fimm u.2019.02298 (2019).
- 4. Zamani, M. R., Aslani, S., Salmaninejad, A., Javan, M. R. & Rezaei, N. Pd-1/Pd-L and autoimmunity: A growing relationship. Cell. Immunol. 310, 27-41, https://doi.org/10.1016/j.cellimm.2016.09.009 (2016).
- 5. Curnock, A. P. et al. Cell-targeted Pd-1 agonists that mimic Pd-L1 are potent T cell inhibitors. JCI Insight 6 https://doi.org/10.117 2/jci.insight.152468 (2021).
- 6. Bryan, C. M. et al. Computational design of a synthetic Pd-1 agonist. Proc. Natl. Acad. Sci. USA 118 https://doi.org/10.1073/pnas .2102164118 (2021).
- 7. Hunt, J. F., Rath, P., Rothschild, K. J., Engelman, D. M. & Spontaneous Ph-dependent membrane insertion of a transbilayer alphahelix. Biochemistry 36, 15177-15192. https://doi.org/10.1021/bi970147b (1997).
- 8. Cheng, C. J. et al. Microrna Silencing for cancer therapy targeted to the tumour microenvironment. Nature 518, 107-110. https:// doi.org/10.1038/nature13905 (2015).
- 9. Son, S. M. et al. Therapeutic effect of phlip-mediated Ceacam6 gene Silencing in lung adenocarcinoma. Sci. Rep. 9, 11607. https:// doi.org/10.1038/s41598-019-48104-5 (2019).
- 10. Reshetnyak, Y. K., Andreev, O. A., Lehnert, U. & Engelman, D. M. Translocation of molecules into cells by Ph-dependent insertion of a transmembrane helix. Proc. Natl. Acad. Sci. USA 103, 6460-6465. https://doi.org/10.1073/pnas.0601463103 (2006).
- 11. Wehr, J. et al. Ph-dependent grafting of cancer cells with antigenic epitopes promotes selective antibody-mediated cytotoxicity. J. Med. Chem. 63, 3713-3722. https://doi.org/10.1021/acs.jmedchem.0c00016 (2020).
- 12. Sun, Y. et al. Ph low insertion peptide-modified programmed cell death-ligand 1 potently suppresses T-cell activation under acidic condition. Front. Immunol. 12, 794226. https://doi.org/10.3389/fimmu.2021.794226 (2021).
- 13. Marusyk, A. & Polyak, K. Tumor heterogeneity: causes and consequences. Biochim. Biophys. Acta. 1805, 105-117. https://doi.org/ 10.1016/j.bbcan.2009.11.002 (2010).
- 14. Fendos, J., Barrera, F. N. & Engelman, D. M. Aspartate embedding depth affects Phlip's insertion Pka. Biochemistry 52, 4595-4604. https://doi.org/10.1021/bi400252k (2013).
- 15. Onyango, J. O. et al. Noncanonical amino acids to improve the ph response of Phlip insertion at tumor acidity. Angew. Chem. Int.
- Ed. Engl. 54, 3658–3663. https://doi.org/10.1002/anie.201409770 (2015).

 16. Coudert, J. D., Scarpellino, L., Gros, F., Vivier, E. & Held, W. Sustained Nkg2d engagement induces cross-tolerance of multiple distinct Nk cell activation pathways. Blood 111, 3571-3578. https://doi.org/10.1182/blood-2007-07-100057 (2008).
- Zak, K. M. et al. Structural biology of the immune checkpoint receptor Pd-1 and its ligands Pd-L1/Pd-L2. Structure 25, 1163-1174 https://doi.org/10.1016/j.str.2017.06.011 (2017).

- Lin, X. et al. Hybrid ferritin nanoparticles as activatable probes for tumor imaging. Angew Chem. Int. Ed. Engl. 50, 1569–1572. https://doi.org/10.1002/anie.201006757 (2011).
- 19. Ji, T. et al. Tumor fibroblast specific activation of a hybrid ferritin nanocage-based optical probe for tumor microenvironment imaging. *Small* 9, 2427–2431. https://doi.org/10.1002/smll.201300600 (2013).
- 20. Certo, M., Tsai, C. H., Pucino, V., Ho, P. C. & Mauro, C. Lactate modulation of immune responses in inflammatory versus tumour microenvironments. *Nat. Rev. Immunol.* 21, 151–161. https://doi.org/10.1038/s41577-020-0406-2 (2021).
- Ivashkiv, L. B. The hypoxia-lactate axis tempers inflammation. Nat. Rev. Immunol. 20, 85–86. https://doi.org/10.1038/s41577-019-0 259-8 (2020).
- 22. Wyatt, L. C., Lewis, J. S., Andreev, O. A., Reshetnyak, Y. K. & Engelman, D. M. Applications of Phlip technology for cancer imaging and therapy. *Trends Biotechnol.* 35, 653–664. https://doi.org/10.1016/j.tibtech.2017.03.014 (2017).
- Cartwright, I. M. et al. Adaptation to inflammatory acidity through neutrophil-derived adenosine regulation of Slc26a3. Mucosal Immunol. 13, 230–244. https://doi.org/10.1038/s41385-019-0237-2 (2020).
- Andreev, O. A. et al. Ph (Low) insertion peptide (Phlip) inserts across a lipid bilayer as a helix and exits by a different path. Proc. Natl. Acad. Sci. USA 107, 4081–4086. https://doi.org/10.1073/pnas.0914330107 (2010).
- Zong, Z., Liu, X., Ye, Z. & Liu, D. A. Double-switch Phlip system enables selective enrichment of Circulating tumor microenvironment-derived extracellular vesicles. *Proc. Natl. Acad. Sci. USA* 120, e2214912120. https://doi.org/10.1073/pnas.2214 912120 (2023).
- 26. Vasquez-Montes, V., Gerhart, J., Thévenin, D. & Ladokhin, A. S. Divalent cations and lipid composition modulate membrane insertion and cancer-targeting action of Phlip. J. Mol. Biol. 431, 5004–5018. https://doi.org/10.1016/j.jmb.2019.10.016 (2019).
- 27. Gupta, C., Ren, Y. & Mertz, B. Cooperative nonbonded forces control membrane binding of the Ph-low insertion peptide Phlip. *Biophys. J.* 115, 2403–2412. https://doi.org/10.1016/j.bpj.2018.11.002 (2018).
- 28. Kyrychenko, A., Vasquez-Montes, V., Ulmschneider, M. B. & Ladokhin, A. S. Lipid headgroups modulate membrane insertion of Phlip peptide. *Biophys. J.* 108, 791–794. https://doi.org/10.1016/j.bpj.2015.01.002 (2015).
- 29. Karabadzhak, A. G. et al. Bilayer thickness and curvature influence binding and insertion of a Phlip peptide. *Biophys. J.* 114, 2107–2115. https://doi.org/10.1016/j.bpj.2018.03.036 (2018).
- 30. Scott, H. L., Heberle, F. A., Katsaras, J. & Barrera, F. N. Phosphatidylserine asymmetry promotes the membrane insertion of a transmembrane helix. *Biophys. J.* 116, 1495–1506. https://doi.org/10.1016/j.bpj.2019.03.003 (2019).
- 31. Westerfield, J. et al. Ions modulate key interactions between Phlip and lipid membranes. *Biophys. J.* 117, 920–929. https://doi.org/10.1016/j.bpj.2019.07.034 (2019).
- 32. Canavan, M., Floudas, A., Veale, D. J. & Fearon, U. The Pd-1:Pd-L1 Axis in inflammatory arthritis. BMC Rheumatol. 5, 1. https://doi.org/10.1186/s41927-020-00171-2 (2021).
- 33. Imagawa, A. & Tachibana, M. Fulminant type 1 diabetes: recent research progress and future prospects. *Diabetol. Int.* 11, 336–341. https://doi.org/10.1007/s13340-020-00466-2 (2020).

Author contributions

H.Z., M.W., J.F. performed the experiments and prepared the manuscript; Y.Z., H.W., M.Z. and X.L. were involved in optimization of the experimental protocols; H.X., C.Q., J.W., L.L., J.F. provided methodological support; Y.Z., Y.W., D.S., G.C. conceived and guided the study.

Funding

This work is supported by the National Natural Science Foundation of China (81672803, 81871252) and the Natural Science Foundation of Inner Mongolia (2022MS08011).

Declarations

Competing interests

The authors declare no competing interests.

Ethical approval

All methods were carried out in accordance with relevant guidelines and regulations. All animal experiments were approved by the Animal Ethics Committee of the Beijing Institute of Pharmacology and Toxicology (IACUC-DWZX-2020-697), and carried out in accordance with Regulations for the administration of affairs concerning experimental animals. The ARRIVE guidelines have been followed for conducting and reporting animal experiments. All experiments involving human subjects were approved by the Ethics Committee of Inner Mongolia Medical University (YKD202201152). All participants were provided with information regarding the study and gave their written informed consent prior to participation. This study was conducted in compliance with the Declaration of Helsinki and all applicable ethical guidelines.

Additional information

Supplementary Information The online version contains supplementary material available at https://doi.org/1 0.1038/s41598-025-98135-4.

Correspondence and requests for materials should be addressed to Y.Z., Y.W., D.S. or G.C.

Reprints and permissions information is available at www.nature.com/reprints.

Publisher's note Springer Nature remains neutral with regard to jurisdictional claims in published maps and institutional affiliations.

Open Access This article is licensed under a Creative Commons Attribution-NonCommercial-NoDerivatives 4.0 International License, which permits any non-commercial use, sharing, distribution and reproduction in any medium or format, as long as you give appropriate credit to the original author(s) and the source, provide a link to the Creative Commons licence, and indicate if you modified the licensed material. You do not have permission under this licence to share adapted material derived from this article or parts of it. The images or other third party material in this article are included in the article's Creative Commons licence, unless indicated otherwise in a credit line to the material. If material is not included in the article's Creative Commons licence and your intended use is not permitted by statutory regulation or exceeds the permitted use, you will need to obtain permission directly from the copyright holder. To view a copy of this licence, visit http://creativecommons.org/licenses/by-nc-nd/4.0/.

© The Author(s) 2025